Supplemental Material S1

TI-IN-ZIRCON THERMOMETRY (ANALYTICAL TECHNIQUE AND ACTIVITY CORRECTIONS)

Trace elements were determined by LA-ICP-MS (Agilent 7500ce quadrupole ICP-MS unit + ESI NWR-193 laser ablation system) located at the NAWI Graz Geocenter - Central Lab Water, Minerals and Rocks, University of Graz and Graz University of Technology, Austria. The spot size of the 193 nm wavelength laser was 35 μm. The laser operated at 8 Hz pulse frequency corresponding to an energy of ~5 mJ cm^{-2}. Ablated material was transported via a helium gas stream (0.75 1 min-1). Standard reference glasses NIST SRM 610 and 612 was routinely analyzed for standardization and drift correction (concentrations from Jochum et al., 2011).

Harvard zircon 91500 with a Ti content of 6 ± 1 ppm (http://georem.mpch-mainz.gwdg.de/sample_query_pref.asp; Yuan et al., 2004; Wiedenbeck et al., 2004) and GZ7 zircon (Nasdala et al., 2018) with a Ti content of 25.1 ± 0.2 ppm were analyzed as unknowns and could be reproduced within given errors for Ti. Silicon (Si) was used as internal standard. Concentrations were calculated from raw data with the Glitter data reduction software (Macquarie, Australia) using the values for NIST610 and 612 from Jochum et al. (2011).

In addition, we make use of LA-ICP-MS zircon analyses done at Boise University (detailed analytical protocol published in Schiller and Finger 2019).

The **correction of Ti and Si activities** is critical for Ti-in-zircon thermometry. Correction values can be retrieved from whole rock chemistry through thermodynamic modelling using rMELTs (Gualda et al. 2012). Schiller and Finger (2019) proposed that the net correction $a_{(TiO2)}/a_{(SiO2)}$ is in the range of 0.5 for most granites, while Volante et al. (2019) reported that they have obtained a better match with T_{Zr} values using an activity correction of 0.9. In this work we have calculated a_{Ti} and a_{Si} values based on rMELTS using the procedure described in Schiller and Finger (2019) (data are given in S2) and the match with T_{Zr} values is satisfactory. We prefer the rMELTS approach relative to that in Volante et al. (2019), because it provides an independent TIZT calculation decoupled from the T_{Zr} calculation.

The **TIZT$_{max}$ values** listed in Tab. 1 were extrapolated from the zircon crystallization temperature distribution curve (Schiller and Finger 2019).

T_{Zr} CALCULATIONS

We used the T_{Zr} calibration of Watson and Harrison (1983) because it appears to be most consistent with melting experiments on granites (see discussion in Schiller and Finger 2019 and Clemens et al. 2021). Considering that granite samples rarely represent fully molten systems (Chappell et al. 1987, Clemens and Stevens 2012) we have corrected the T_{Zr} values assuming 85 % (by weight) melt fraction. This is a reasonable general approach according to thermodynamic modelling (Schiller and Finger 2019).

MORPHOLOGICAL AND CL-BASED ZIRCON ANALYSIS AS AN IMPORTANT TOOL FOR MULTI-ASPECTUAL ZIRCON THERMOMETRY

Not every zircon in a granitic rock precipitated from the melt phase. Especially "cold" granites (Miller et al. 2003, Bea et al. 2021) may carry large amounts of inherited (entrained) zircon from the source that did not dissolve in the magma (Clemens and Stevens 2012). Granites may occasionally also contain large amounts of xenocrystic zircon derived from country rocks (Finger et al. 1991). Differentiated granites may contain antecrystic zircon from the precursor magma that was not fractionated out. Also, hybrid magmas may carry antecrystic zircon entrained from the mafic magma.

All these non-autocrystic zircons exert severe complications for zircon thermometry (Siegel et al 2019). Their abundance in a granite should always be semi-quantitatively estimated (Tab. 1).

Zircon mounts, as routinely prepared for LA-ICP-MS analysis, can be perfectly used to examine a zircon population with reference to inherited, xenocrystic or antecrystic components. An important prerequisite is that the mount contains a random selection of zircons that is representative for the granite sample.

If the zircon grains are embedded in transparent resin, optical microscopy is a first useful step of investigation. It allows a detailed morphological analysis of the zircon population (Poldervaart 1950, Frasl 1963, Hoppe 1963, Pupin 1980). Zircons that precipitate from a cooling granitic melt (also termed autocrystic, newly-formed or N-type in the literature - Finger et al. 1991), commonly display a distinct, well-defined morphology in terms of crystal size, elongation and tracht. These morphological features are determined by the physical and chemical magmatic crystallization conditions (Benisek and Finger 1993) and systematically different in different granite types (Frasl 1963, Pupin 1980). Morphological outliers are thus always candidates for xenocrysts or antecrysts (Finger et al. 1991). A typical sign for zircon inheritance are zoned zircons with rounded resorbed cores (Corfu et al. 2003). This feature is best observed in cathodoluminescence (CL) images.

CL imaging is today routinely done in the forefield of a LA-ICP-MS zircon study, with the aim to place the analyses points precisely into crack- and inclusion-free, genetically coherent crystal domains. Cathodoluminescence imaging and U-Pb dating are powerful methods to assess the rate of zircon inheritance in a granite.

For Ti-in-zircon thermometry measurements in autocrystic zircon domains (normally with fine, euhedral oscillatory zoning) are relevant. Zircon analyses with an anomalous trace element signal may hint at potential xenocrysts or antecrysts and should be sorted out. Likewise, sector-zoned zircon domains that indicate a chemical disequilibrium, and patchy recrystallization zones are to be avoided.

The above mentioned methods of investigation will mostly allow a good estimate to what extent a granite carries autocrystic, inherited, xenocrystic and eventually antecrystic zircons (see the following table). If autocrystic zircons make up less than 80 vol.% of all zircon, T estimates with the zircon solubility model could be problematic (see sample JZ262). Our study confirms earlier findings (Miller et al. 2003) that this problem will mainly concern LT and VLT granites.

Selected CL images

Some examples of inherited and xenocrystic zircon grains are shown here. The non-autocrystic origin of these grains is evidenced by an increased U-Pb age.
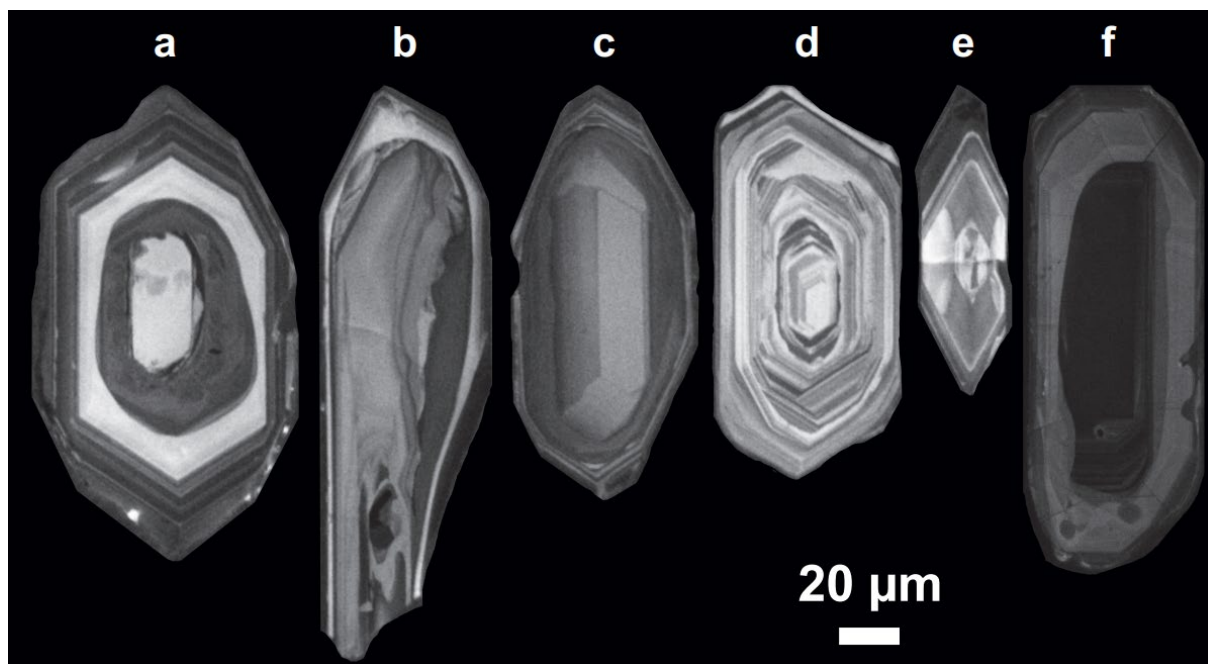
Figure S1. a-b) Zircons from Weinsberg Granite II with inherited cores.
c-e) Xenocrystic zircons with only thin autocrystic overgrowths (Freistadt granodiorite)
f) Zircon with inherited core from UHT granite sample HL 34 (LOG).

## Table S1. Multi-aspectual zircon thermometry protocol including zircon morphology data

| Sample | Unit | T-Class. | T_{Zr} | TIZT | | Zircon population analysis | | | | Under-satur. |
				Av.-T	$TIZT_{Max}$	Inh	Xen	Ant	Typical Morphology of Autocrysts	
Fi 1 19	WBG I	**HT**	862	817±37	871	5	n.e.	n.e.	L80-220 E3-5; *S19-20, S24-25*	n.e.
JZ 262	ESG II	MT (?)	807 (?)	781±39	831	50	10	n.e.	L80-140 E2-4; *L2, S1, S2*	likely
Fi 84 08	ESG III	**MT-HT**	843	830±37	877	5	5	n.e.	L60-150 E2-3; *S1, S2, S6*	n.e.
Fi 13 18	WBG II	**MT**	832	802±26	845	5	n.e.	n.e.	L120-350 E2-4; *S2, S3, S7, S8*	n.e.
KJ 18	WBG II	**MT**	850	789±35	831	10	n.e.	n.e.	L80-250 E2-6; *S2, S3, S7, S8*	n.e.
KV 829	WBG II	**MT**	851	790±35	838	10	n.e.	n.e.	L150-400 E2-5; *S2, S3, S7, S8*	n.e.
Fi 15 85	WBG III	**HT**	855	837±44	888	5	n.e.	n.e.	L90-200 E1-3; *S13-14, S19-20*	n.e.
Fi 20 86	WBG III	**UHT**	919	879±31	929	5	n.e.	n.e.	L50-180 E2-5; *S19-20, S24-25*	n.e.
SD 24 17	WBG III	**HT**	870	819±34	867	5	n.e.	n.e.	L50-200 E1-5; *S19-20, S24-25*	n.e.
SD 38 11	LOG	**UHT**	948	887±49	937	5	n.e.	n.e.	L50-120 E2-4; *S19-20, S24-25*	n.e.
HL 14a	LOG	**UHT**	927	922±32	966	5	n.e.	n.e.	L90-150 E2-4; *S12-13, S17-18*	n.e.
HL 34	LOG	**UHT**	904	913±33	940	5	n.e.	n.e.	L80-150 E1-3; *S19-20, S24-25*	n.e.
BB 3	LOG	**UHT**	908	831±57	902	5	n.e.	n.e.	L80-170 E2-4; *S20, S24, S25*	n.e.
Fi 92 81	LOG	**UHT**	941	858±60	945	10	n.e.	n.e.	L50-280 E2-5; *S6, S7, S11, S12*	n.e.
ML 19 01	FRG	**LT**	796	739±29	787	n.e.	10	n.e.	L80-180 E3-6; *G1, L2-L5*	n.e.

Abbreviations: n.e. = no evidence, L=Length (in µm), E=Elongation (length/width).
Columns labelled Inh, Xen, Ant give the estimated proportions of inherited, xenocrystic and antecrystic zircons (in vol.% of all zircons).
Definition of forms (italics, e.g. *S12*) is according to Pupin (1980). See diagram below.

Figure S2. Pupin diagram
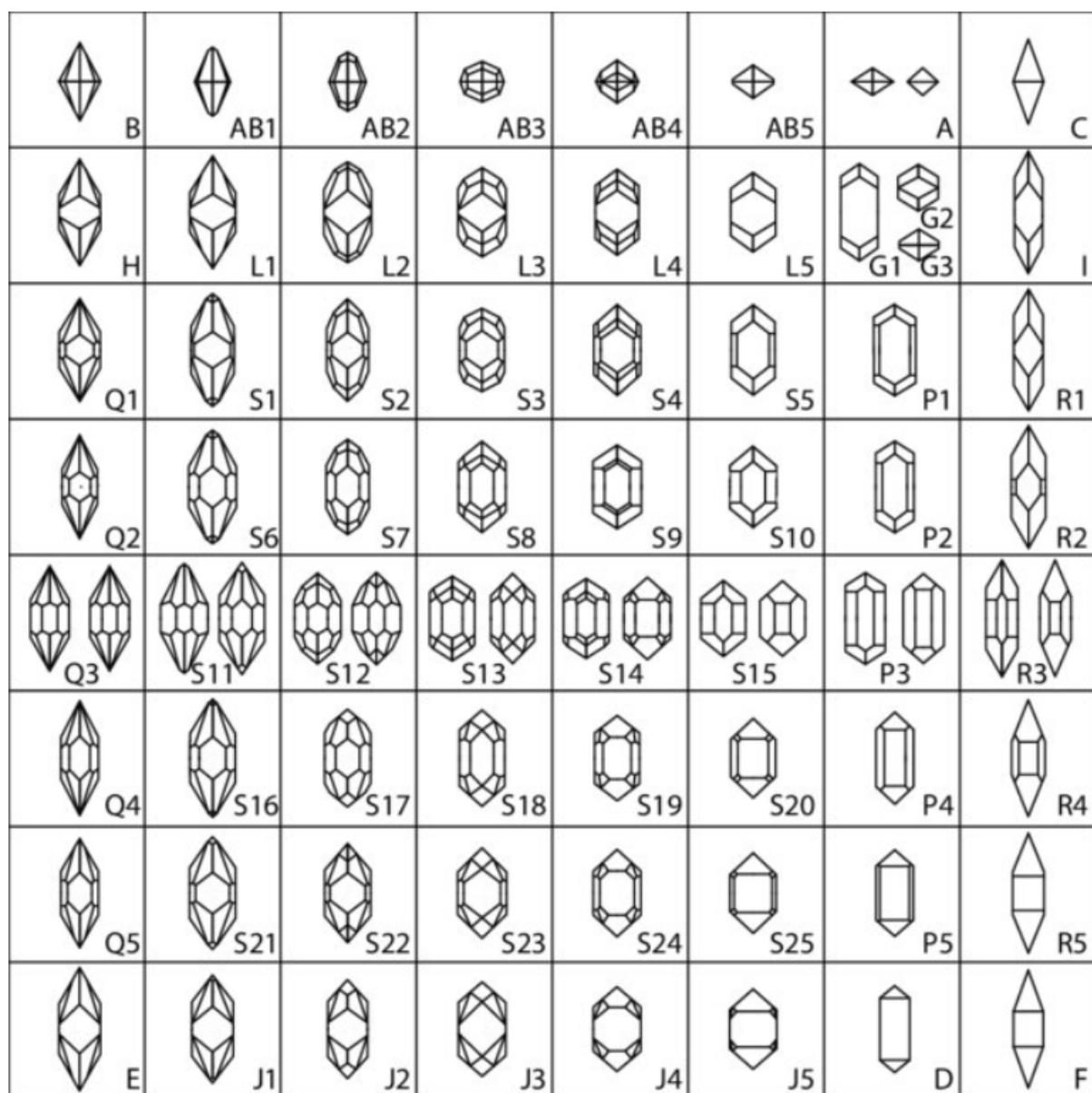
References S1

Benisek, A., Finger, F., 1993, Factors controlling the development of prism faces in granite zircons: a microprobe study: Contrib. Mineral. Petrol., v. 114, p. 441-451.

Clemens, J.C., Stevens, G., Mayne, M.J., 2021, Do arc silicic magmas form by fluid-fluxed melting of older arc crust or fractionation of basaltic magmas? Contrib. Mineral. Petrol. 176,

Corfu, F., Hanchar, J.M., Hoskin, P.W.O., and Kinny, P. 2003, Atlas of Zircon Textures: Reviews in Mineralogy and Geochemistry v. 53(1), p. 469-500.

Finger, F., Friedl, G., Haunschmid, B., 1991, Wall-rock-derived zircon xenocrysts as important indicator minerals of magma contamination in the Freistadt granodiorite pluton, northern Austria: Geol. Carpathica, v. 42/2, p. 67-75.

Frasl, G., 1963, Die mikroskopische Untersuchung der akzessorischen Zirkone als eine Routinearbeit des Kristallingeologen: Jb.Geol.B.-A., v.106, p. 405-428.

Gualda, G.A., Ghiorso, M.S., Lemons, R.V., and Carley, T.L., 2012, RhyoliteMELTS: a modified calibration of MELTS optimized for silica rich, fluid-bearing magmatic systems: J. Petrol., v. 53, p. 875–890.

Hoppe, G., 1963, Die Verwendbarkeit morphologischer Erscheinungen an akzessorischen Zirkonen für petrogenetische Auswertungen: Abh. dt. Akad. Wiss. KI. Bergbau etc.,1963/1, 130p.

Nasdala, L., Corfu, F., Schoene, B., Tapster, S.R., Wall, C.J., Schmitz, M.D., Ovtcharova, M., Schaltegger, U., Kennedy, A.K., Kronz, A., Reiners, P.W., Yang, Y.-H., Wu, F.-Y., Gain, S.E.M., Griffin, W.L., Szymanowski, D., Chanmuang, C., Ende, M., Valley, J.W., Spicuzza, M.J., Wanthanachaisaeng, B. and Giester, G., 2018, GZ7 and GZ8 – Two Zircon Reference Materials for SIMS U-Pb Geochronology: Geostandards and Geoanalytical Research. doi: 10.1111/ggr.12239

Poldervaart, A., 1955, Zircons in rocks: Am. Jour. Sci., v. 253, p. 433-461.

Pupin, J.P., 1980, Zircon and granite petrology: Contrib. Min. Petr., v. 73, p.207-220.

Schiller, D., and Finger, F., 2019, Application of Ti-in-zircon thermometry to granite studies: problems and possible solutions: Contrib. Mineral. Petrol., v. 174, p. 51.

Yuan, H., Gao, S., Liu, X., Li, H., Günther, D. and Wu, F., 2004, Accurate U-Pb Age and Trace Element Determinations of Zircon by Laser Ablation-Inductively Coupled Plasma-Mass Spectrometry: Geostandards and Geoanalytica Research, v. 28, p. 353-370.

Wiedenbeck, M., Hanchar, J.M., Peck, W.H., Sylvester, P., Valley, J., Whitehouse, M., Kronz, A., Morishita, Y., Nasdala, L., Fiebig, J., Franchi, I., Girard, J.P., Greenwood, R.C., Hinton, R., Kita, N., Mason, P.R.D., Norman, M., Ogasawara, M., Piccoli, P.M., Rhede, D., Satoh, H., Schulz-Dobrick, B., Skår, Ø., Spicuzza, M.J., Terada, K., Tindle, A., Togashi, S., Vennemann, T., Xie, Q. and Zheng, Y.F., 2004, Further Characterisation of the 91500 Zircon Crystal: Geostandards and Geoanalytical Research, v. 28, p. 9-39.

DATA SOURCES FOR T$_{Zr}$ THERMOMETRY

Bayer, B., 2016, Geochemische Untersuchungen in der Übergangszone von Weinsberger Granit zu Schlierengranit bei Hirschbach im Mühlviertel (Oberösterreich): MSc Thesis Univ. Salzburg, 83 p.

Breiter, K., 2010, Geochemical classification of Variscan Granitoids in the Moldanubicum (Czech Republic, Austria): Abh. Geol. B.-A., v. 65, p. 19–25.

Breiter, K., and Koller, F. (1999): Two Mica Granites in the Central Part of the South Bohemian Pluton.- Abh. Geol. B.-A., 56/1: 201-212; Wien.

Breiter, K. und Scharbert, S., 1998, Latest Intrusions of the Eisgarn Pluton (South Bohemia - Northern Waldviertel): Jb. Geol. B.-A., v. 141 H.1, p. 25-37

Finger, F., 1984, Die Anatexis im Gebiet der Donauschlingen bei Obermühl (Oberösterreich). – PhD Thesis Univ. Salzburg, 217 p.

Frasl, G., and Finger, F., 1991, Geologisch-petrographische Exkursion in den österreichischen Teil des Südböhmischen Batholiths: Eur.J.Mineral., v. 3, Bh 2, p. 23-40.

Gerdes, A., 1997, Geochemische und thermische Modelle zur Frage der spätorogenen Granitgenese am Beispiel des Südböhmischen Batholiths: Basaltisches underplating oder Krustenstapelung? PhD thesis Math. Naturw. Fak. d. Georg Aug. Univ. Göttingen, 130 p..

Krenn E., 2000, Zur Petrologie und Geologie der sogenannten Migmagranite des Südböhmischen Batholiths: MSc. Thesis Univ. Salzburg, 93 p.

Leitich A., Der feinkörnige Granit von Tragwein im unteren Mühlviertel (Oberösterreich, Böhmische Masse): MSc Thesis Univ. Salzburg, 95 p.

Liew, T.C., Finger, F., and Höck, V., 1989, The Moldanubian granitoid plutons of Austria: chemical and isotopic studies bearing on their environmental setting: Chem. Geol., v. 76, p. 41–55.

Lindschinger, H., 2014, Geologie und Petrographie eines komplexen Granitprofils in der Bavarischen Zone der Böhmischen Masse (Kartenblatt Freistadt, Oberösterreich): MSc. Thesis, University of Salzburg, 87p.

René, M., Holtz, F., Luo, C., Beermann, O., Stelling, J., 2008, Biotite stability in peraluminous granitic melts: compositional dependence and application to the generation of two-mica granites in the South Bohemian Batholith (Bohemian Massif, Czech Republic); Lithos v. 102, p. 538–553.

René, M., 2016, Source compositions and melting temperatures of the main granitic suites from the Moldanubian Batholith: Journal of Geosciences, v. 61, p. 355 – 370.

Schiller, D., 2013, Der Steinberg Granit des Plöckenstein Massivs (nordwestliches Mühlviertel): MSc Thesis Univ. Salzburg, 119 p.

Vellmer, C., 1992, Stoffbestand und Petrogenese von Granuliten und granitischen Gesteinen der südlichen Böhmischen Masse in Niederösterreich: PhD thesis Georg Aug. Univ. Göttingen, 111 p.
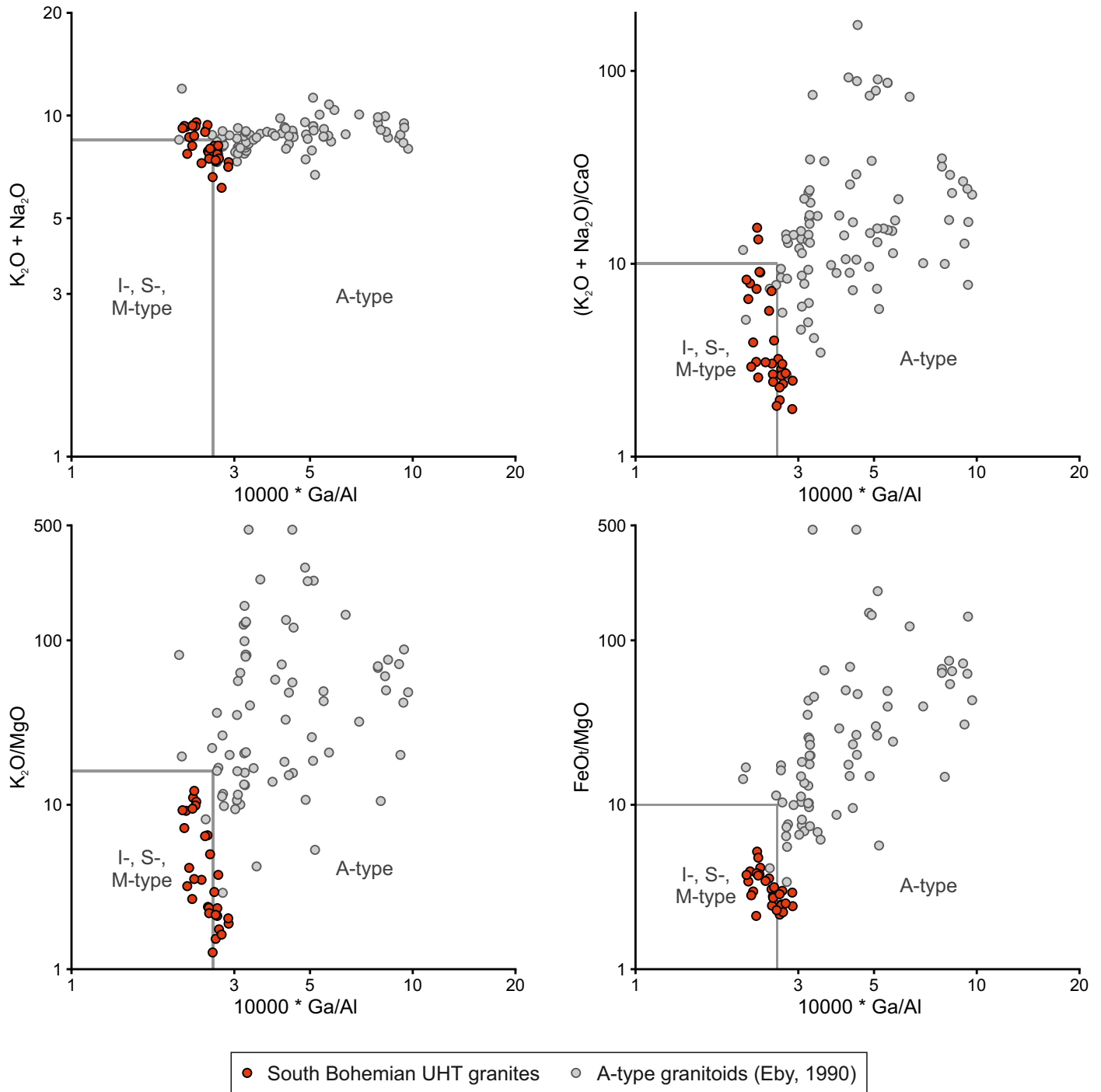
Sample	Main Reference
Fi 1 19	Gerdes 1997
JZ 262	Univ. Salzburg data unpubl.
Fi 84 08	Schiller 2013
Fi 13 18	Gerdes 1997
KJ 18	Univ. Salzburg data unpubl.
KV 829	Schiller and Finger 2019
Fi 15 85	Gerdes 1997
Fi 20 86	Gerdes 1997
SD 24 17	Schiller 2013
SD 38 11	Schiller 2013
HL 14a	Lindschinger 2014
HL 34	Lindschinger 2014
BB 3	Bayer, 2016
Fi 92 81	Finger 1984
ML 19	Univ. Salzburg data unpubl.

Supplemental Material S3

SiO$_2$ vs Zr diagrams for the South Bohemian Batholith
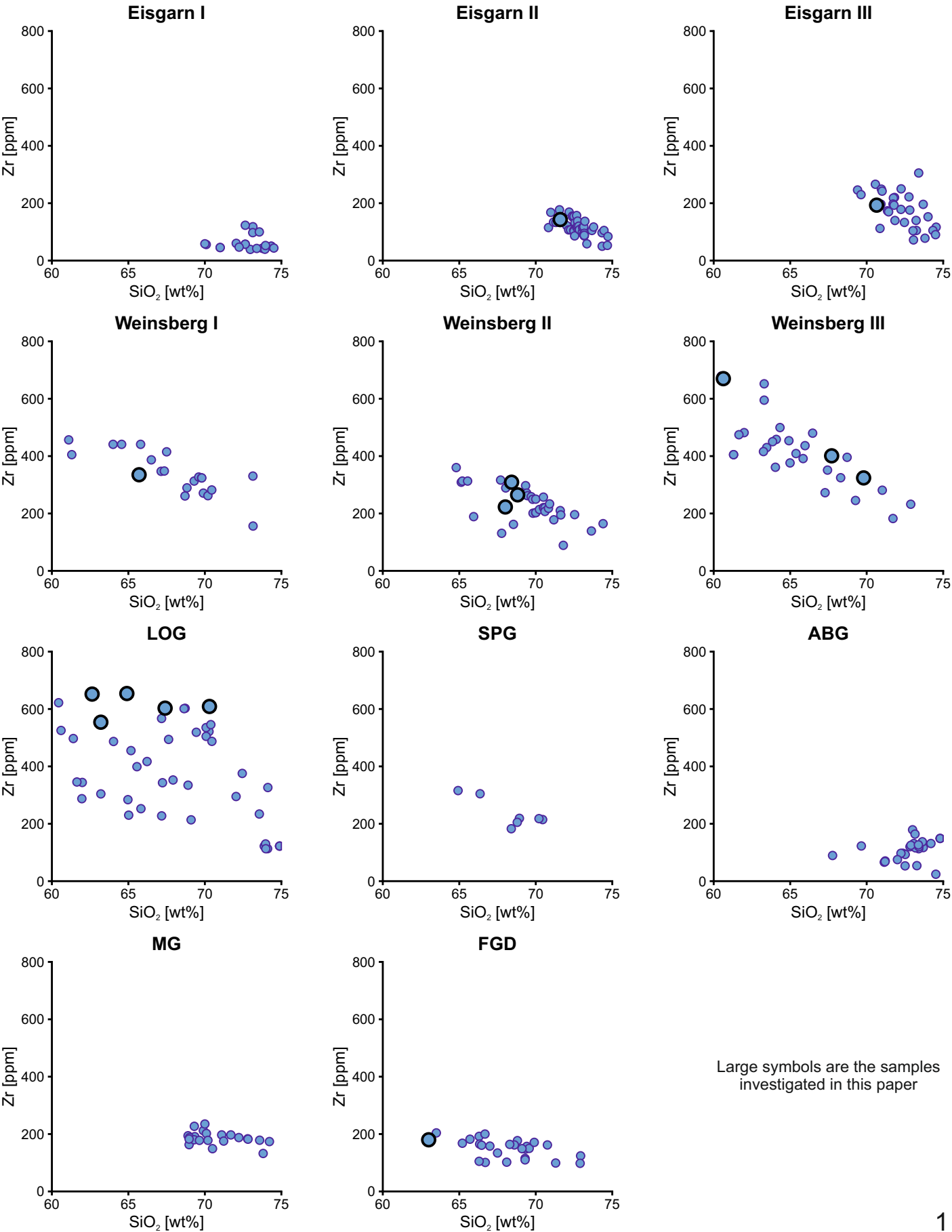
Large symbols are the samples investigated in this paper

Diagrams from Whalen et al. (1987) showing a comparison between the South Bohemian Batholith UHT granites and A-type grantites (Eby, 1990).
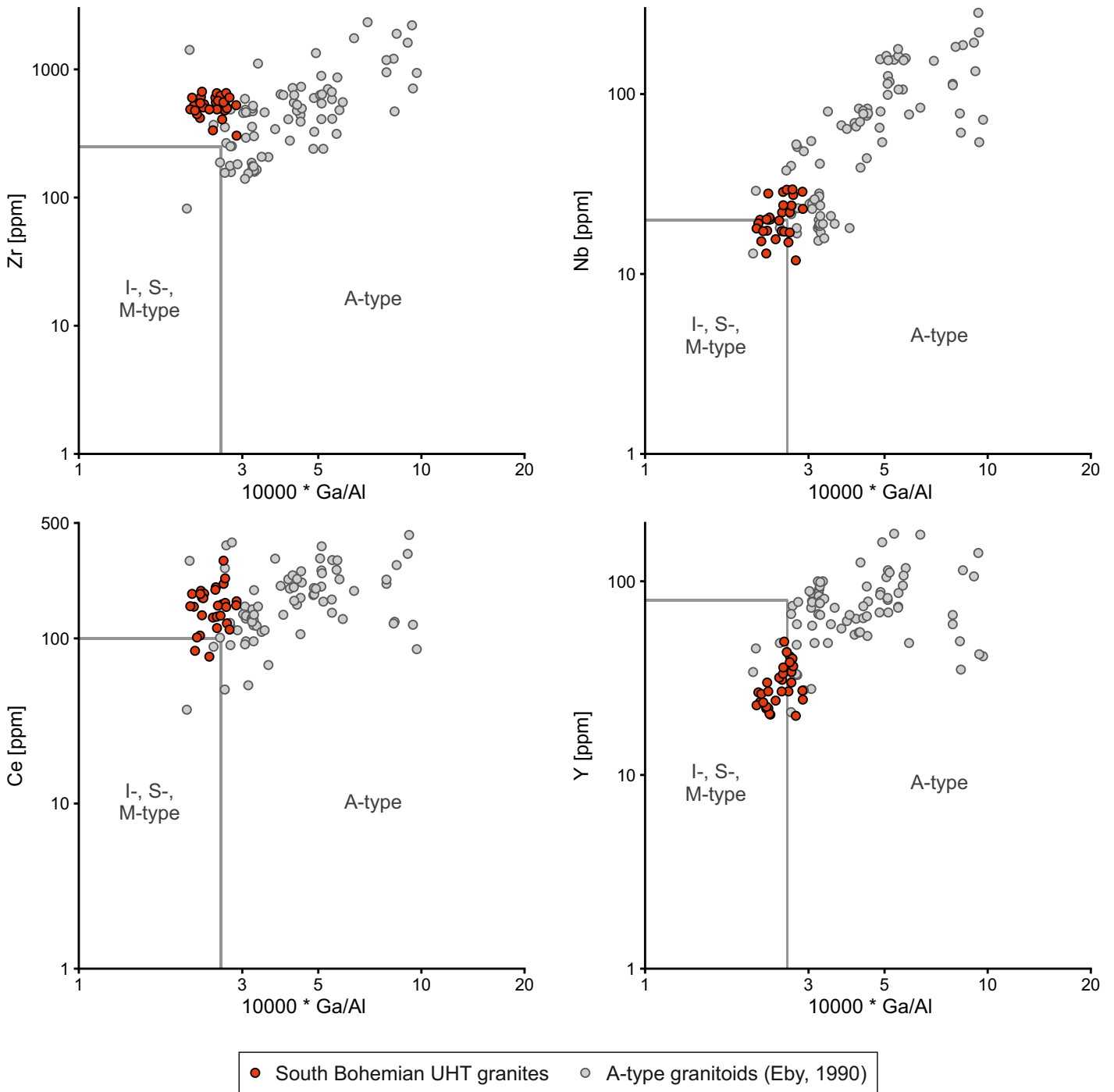
References:
Eby, G.N., 1990, The A-type granitoids: A review of their occurrence and chemical characteristics and speculations on their petrogenesis: Lithos, v. 26, p. 115134, doi:10.1016/0024-4937(90)90043-Z.

Whalen, J.B., Currie, K.L., and Chappell, B.W., 1987, A-type granites: geochemical characteristics, discrimination and petrogenesis: Contributions to Mineralogy and Petrology, v. 95, p. 407419, doi:10.1007/BF00402202.

Diagrams from Whalen et al. (1987) showing a comparison between the South Bohemian Batholith UHT granites and A-type grantites (Eby, 1990).

References:
Eby, G.N., 1990, The A-type granitoids: A review of their occurrence and chemical characteristics and speculations on their petrogenesis: Lithos, v. 26, p. 115134, doi:10.1016/0024-4937(90)90043-Z.

Whalen, J.B., Currie, K.L., and Chappell, B.W., 1987, A-type granites: geochemical characteristics, discrimination and petrogenesis: Contributions to Mineralogy and Petrology, v. 95, p. 407419, doi:10.1007/BF00402202.